

HNAS: Hierarchical Neural Architecture Search on Mobile Devices

Xin Xia Wenrui Ding

Beihang University

Abstract. Neural Architecture Search (NAS) has attracted growing interest. To reduce the search cost, recent work has explored weight sharing across models and made major progress in One-Shot NAS. However, it has been observed that a model with higher one-shot model accuracy does not necessarily perform better when stand-alone trained. To address this issue, in this paper, we propose a new method, named Hierarchical Neural Architecture Search (HNAS). Unlike previous approaches where the same operation search space is shared by all the layers in the supernet, we formulate a hierarchical search strategy based on operation pruning and build a layer-wise operation search space. In this way, HNAS can automatically select the operations for each layer. During the search, we also take the hardware platform constraints into consideration for efficient neural network model deployment. Extensive experiments on ImageNet show that under mobile latency constraint, our models consistently outperform state-of-the-art models both designed manually and generated automatically by NAS methods.

Keywords: Neural architecture search, weight sharing, operation pruning, mobile devices

1 Introduction

Neural Architecture Search (NAS) has received increasing attention in both industry and academia, and demonstrated much success in various computer vision tasks, such as image recognition [15,22,40,41], object detection [9,33], and image segmentation [6,21,26]. Early work [40,41] is mainly built on top of reinforcement learning (RL) [34], where tremendous amount of time is needed to evaluate candidate models by training them from scratch. In [29], the authors use evolutionary algorithm (EA) and achieve comparable result to RL. Recently, more and more researchers have adopted weight sharing approaches [4,22,27,36,39] to reduce the computation. They utilize an over-parameterized network, which is defined to subsume all architectures and needs to be trained only once.

Weight-sharing approaches can be mainly divided into two categories. In the first category, researchers use a continuous relaxation of search space [5,22,35]. The architecture distribution is continuously parameterized. Supernet training and architecture search are deeply coupled into single stage and jointly optimized by gradient based methods. Deep coupling between the architecture parameters

and supernet weights introduces bias and instability to the search process. One-Shot NAS [3,4,10,15] belongs to the other category. The optimization of the supernet weights and architecture parameters are decoupled into two sequential steps. The fairness among all architectures is ensured by sampling architecture or dropping out operators uniformly. During the architecture search, the validation accuracy of a model is predicted by inheriting the weights from the trained supernet. Unfortunately, as stated in [2,3,10], weight coupling issue exists in one-shot methods that one-shot model accuracy can not truly reflect the relative performance of architectures.

In this paper, we aim to address weight coupling issue in one-shot approaches from the view of operation search space. Current one-shot approaches [3,4,10,15] use the same operation search space for all the layers. However, in practice, we observe some operations will never be selected by certain layers in the final architectures. The reason is sub-networks that contain these redundant operations either violate the hardware platform constraints, or perform poorly on the validation dataset and are excluded during the architecture search. So a natural question arises: if an operation will never be selected, why spend the effort on training it at the very beginning? Keeping these operations will degrade the performance of One-Shot NAS, since the more operations, the more severe the interference between the operations. Thus, an effective way to mitigate the weight coupling is to remove these operations before training. A follow-up question is how we can identify if an operations is redundant or not, before the training of a supernet.

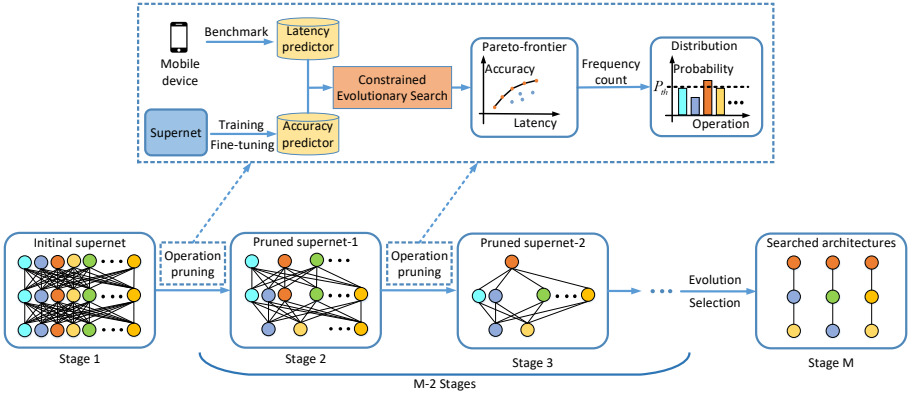


Fig. 1. The overall framework of HNAS. **Bottom:** HNAS is divided into M stages: the first stage is initial supernet training, and the next $M-2$ stages repeat the process of pruning the operations and training the pruned supernet. The last stage is the architecture evolution and selection. **Top:** The procedures of operation pruning. Supernet is used as an accuracy predictor after training, and a latency predictor is built for target mobile devices. The constrained evolutionary search algorithm is used to evolve the network architecture, and the probability distribution of the operations for each layer is estimated from Pareto frontier.

To answer the questions above, we propose a simple yet effective approach named Hierarchical Neural Architecture Search (HNAS). Our algorithm can automatically select its own operations for each layer and build a layer-wise search space through hierarchical search strategy. The flow of our algorithm is illustrated in Fig. 1. In the first stage, we perform the training of an initial supernet, where the operation search space is shared by all the layers. For the next $M-2$ stages, we start from the supernet coming from the previous stage, and estimate the operation probability distribution for each layer from the architectures that reside on the Pareto frontier [14]. Next, we prune the operations layer by layer and remove the ones whose probabilities are below certain threshold to build the pruned supernet for the next stage. Finally, we finetune the pruned supernet. We repeat the process above until stopping criterion is satisfied. In the final stage, we search the architectures from the supernet and return the architectures with highest accuracy.

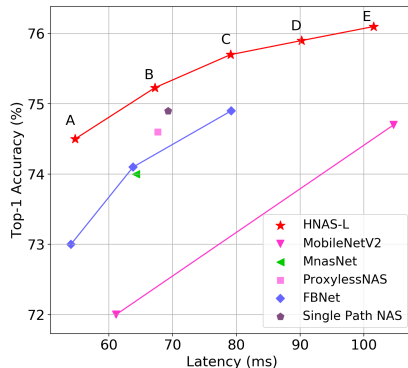


Fig. 2. The trade-off between Pixel 3 latency and top-1 ImageNet accuracy. All models use the input resolution 224 and the latency is measured on a single large core of the same device using TFLite[1].

The effectiveness of HNAS is demonstrated on ImageNet. We name the models discovered by HNAS as HNASs. HNASs surpass state-of-the-art (SOTA) efficient networks designed manually and automatically, such as MobileNetV2 [30], FBNet [35], ProxylessNAS [5] and SPOS [15], without sacrificing mobile efficiency. As shown in Fig. 2, HNAS-L-A achieves 74.5% top-1 accuracy with 271M FLOPs and 54.7 ms latency on an Pixel 3 phone, 1.5% higher than FBNet-A [35]. Top-1 accuracy of HNAS-L-B is 0.6% higher than Proxyless-R [5], while HNAS-L-C achieves 0.8% absolute gain in top-1 accuracy compared with FBNet-C [35]. Our main contributions are summarized as follows:

- We present HNAS, an efficient neural architecture search framework for One-Shot NAS. It returns the searched networks gradually through a hierarchical search strategy.
- We develop an operation pruning method for One-Shot NAS. As far as we know, this is the first attempt to bring pruning into One-Shot NAS. It removes unnecessary operations for each layer and reduces the search space.

- To our best knowledge, we are the first to automatically build layer-wise operation search space for One-Shot NAS.
- Our proposed HNAS is hardware-aware. Various hardware platform constraints can be incorporated into the search, such as latency, FLOPs, and the number of parameters in the architecture.
- Extensive experiments demonstrate the advantage of HNAS. It achieves SOTA performance on ImageNet and mitigates weight coupling.

2 Related Work

Recently, in order to reduce the computation cost of NAS, some researchers propose weight sharing approaches to speed up the architecture search, such as ENAS [27], DARTS [22], and One-Shot NAS [3,15]. All sub-network architectures inherit the weights from the trained supernet without training from scratch. DARTS softens the discrete search space into a continuous search space and directly optimizes it by the gradient method. [4] and [3] proposes a method which decouples supernet training and architecture search into two sequential stages, including supernet training and architecture search. However, due to the weight coupling in the supernet, the accuracy of the supernet prediction has a certain deviation from the ground truth, which result in inaccurate ranking of the architectures. The authors of SPOS [15] further propose uniform sampling and single-path training to overcome weight coupling in One-Shot NAS. ProxylessNAS [5] binarize entire paths and keep only one path when training the over-parameterized supernet to reduce memory footprint. FBNet [35] use a proxy dataset (subset of ImageNet) to train the continuously parameterized architecture distribution. FairNas [10] is based on [15] and proposes a new fairness sampling and training strategy for supernet training.

Different from the methods above, we propose a hierarchical search strategy to gradually reduce the number of operations in each stage and build a layer-wise operation search space for One-Shot NAS automatically. Our work is most closely related to [8] and [38]. In [8], the authors propose a progressive version of DARTS to bridge the depth gap between search and evaluation scenarios. Its core idea is to gradually increase the depth of candidate architectures. The authors of [38] aim to address the challenge of hardware diversity in NAS. They design the hardware-aware search space manually by sorting the scores of each operation by its FLOPs, latency and number of parameters.

Another relevant topic is network pruning [16,17,23] that aim to reduce the network complexity by removing redundant, non-informative connections in a pre-trained network. Similar to this work, we start from an over-parameterized supernet and then prune the redundant operations to get the optimized architecture. The distinction is that they aim to prune the connections in a pre-trained network, while we focus on improving One-Shot NAS performance through operation pruning.

3 Method

3.1 Problem Formulation and Motivation

One-Shot NAS [3,4] contains two stages. The first stage is supernet training, which is formulated as:

$$W_S = \arg \min_W \text{Loss}_{train}(N(S, W)), \quad (1)$$

where $\text{Loss}_{train}(\cdot)$ is the loss function on the training set, $N(S, W)$ is the supernet, represented by the search space S and its weights W , and W_S are the learned weights of the supernet.

The second stage is the architecture search. It aims to find the architectures from the supernet that has the best one-shot accuracy on the validation set under mobile latency constrain, expressed as:

$$\begin{aligned} s^* &= \arg \max_{s \in S} \text{Acc}_{val}(N(s, W_S(s))) \\ s.t. & \text{Lat}_{\min} \leq \text{Latency}(s^*) \leq \text{Lat}_{\max}, \end{aligned} \quad (2)$$

where Lat_{\min} and Lat_{\max} are lower and upper mobile latency constraint. Each sampled sub-network inherits its weights from W_S as $W_S(s)$. Therefore, one-shot accuracy $\text{Acc}_{val}(\cdot)$ only requires inference on validation dataset. This completes the search phase. In the evaluation phase, without violating the mobile latency constraint, the architectures with the highest one-shot accuracy will be selected to do the stand-alone training from scratch.

However, as stated by many researchers [3,4,15], weight coupling issue exists in One-Shot NAS, which results in ranking inconsistency between supernet predicted accuracies and that of ground-truth ones by stand-alone training from scratch. Architectures with a higher supernet predicted accuracy during the search phase may perform worse in the evaluation phase.

In this paper, we aim to mitigate weight coupling and improve the performance of One-Shot NAS. We start with the analysis of operation search space. In practice, we observe that redundant operations exist in the supernet. These redundant operations will never be selected by the searched architectures. As shown in Fig. 3, where x-axis represents the layer name and y-axis represents the operation name, the operation distribution in each layer is sparse. For example, in layer1, the distribution concentrates on the operation IBconv_K3_E1, while all the other operations never appear in this layer. The reason lies in the architectures that contain the redundant operations either violate the constrains in Eq. 2, or has a low validation accuracy and are excluded during the architecture search.

Motivated by [16] where uncritical connections in deep networks can be removed without affecting the performance, we claim that existing operation search space is redundant, and needs to be pruned. However, different from network pruning [16], whose main purpose is to decrease the network complexity, our

main goal is to mitigate weight coupling and improve One-Shot NAS performance by pruning unnecessary operations. These operations will hurt the supernet training since more operations means more intense interference between the operations in the supernet, resulting in more severe ranking inconsistency between supernet predicted accuracy and ground-truth one. However, large number of operations is demanded for NAS to discover promising models. Due to this conflict, we present HNAS which follows a coarse-to-fine manner to refine the operation search by gradually pruning the operations and build the layer-wise operation search space automatically.

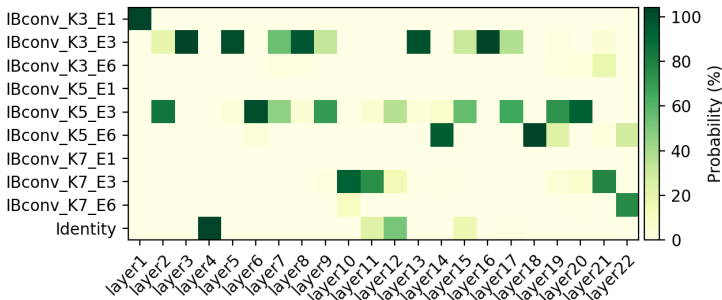


Fig. 3. Probability distribution of each layer’s operation in the searched architectures.

3.2 Hierarchical Neural Architecture Search

The whole process of HNAS is elaborated in Algorithm 1. $s^{i,j}$ denotes the i th operation for layer j in the supernet, $p^{i,j}$ represents the probability of operation $s^{i,j}$. We start with an initial operation search space, which is shared by all the layers in the supernet. Next, we construct the supernet following Table 1 with this initial search space and train it with path-wise manner proposed in [15]. This is the first stage of HNAS, served as the initialization. For the next $M-2$ stages, we first use constrained evolutionary algorithm to search the architectures that belong to Pareto frontier on the input supernet. The output supernet of the previous stage is fed as the input of the current stage. Then, we estimate the probability distribution of each operation layer-by-layer from Pareto frontier and remove the operations whose probabilities are below certain threshold P_{th} . To this end, we build the layer-wise operation search space for the current stage. The last part is to finetune the pruned supernet and feed it into the next stage. The process above is repeated until we reach the targeted number of search stages. When it comes to the last stage of HNAS, constrained evolutionary algorithm is used to search the architectures on the supernet, which is the output of the $(M-1)$ th stage, and return the architectures with highest accuracy. We list more details as follows.

Algorithm 1 Hierarchical Neural Architecture Search

Input: operation search space $S = \{s^{i,j}\}$, probability threshold P_{th} , the number of hierarchical search stages M , latency constraints Lat_{min} and Lat_{max} , and the number of layers J in the supernet

- 1: Initial supernet training: construct and train supernet $N(S, W)$
 - 2: **for** $k = 2$ to $M - 1$ **do**
 - 3: Architecture search: search the architectures on the supernet $N(S, W)$
 - 4: **for** $j = 1$ to J **do**
 - 5: Distribution estimation: count and normalize the frequency of $s^{i,j}$ to get $p^{i,j}$
 - 6: **end for**
 - 7: Pruning: remove $s^{i,j}$ from S if $p^{i,j} < P_{th}$
 - 8: Pruned supernet training: construct and finetune supernet $N(S, W)$
 - 9: **end for**
 - 10: Repeat step 3
 - 11: **return** the architectures with highest accuracy
-

Initial Supernet Training. For the training of initial supernet, we adopt a path-wise [15] manner, where supernet training and architecture search are decoupled into two sequential steps, to ensure the trained supernet can reflect the relative performance of sub-networks. However, since weight coupling is inevitable in weight-sharing approaches [15,22], supernet predicted accuracy can only coarsely indicate the relative ranking of sub-networks. The trained initial supernet is the starting point of HNAS and served as the initialization.

Constrained Evolutionary Search. After initial supernet training, we need to search the architectures. Evolutionary search performs better than random search in previous one-shot works [3,4,15]. The evolutionary algorithm is flexible in dealing with hardware platform constraints in Eq. 2, since the mutation and crossover processes can be manipulated to generate proper candidates to satisfy the constraints. We aim to estimate the probability distribution of operations by counting their frequencies in the searched architectures. The estimated operation distribution is unstable and exhibits a large variance if the evolutionary search algorithm in [15] is used.

To deal with this problem, we propose Constrained Evolutionary Search (CES), which is built on top of Non-Dominated Sorting Genetic Algorithm II (NSGA-II) [12]. Note that the authors of [24] are the first to introduce NSGA-II into NAS. Architecture search can be formulated as a multi-objective optimization problem to balance between mobile latency and architecture accuracy. We add latency constraint into the iteration of NSGA-II to formulate CES. More specifically, we discard the architectures that violate the constraint in the crossover and mutation of CES. This change gives us better result. Different from the evolutionary search in [15] that architectures with poor accuracy are discarded in each iteration, no architectures are discarded but all of them are sorted by its latency and accuracy in each iteration. The estimated operation distribution by CES is stable and its corresponding variance is small.

During the search, the architecture accuracy is predicted by the supernet through weight inheritance, and its corresponding latency on mobile devices is estimated by the latency predictor. We build a lookup table of mobile latency for operations in the supernet and the architecture latency is predicted by summing up the latency of all of its operations.

Operation Pruning. We prune the operations based on its corresponding probability distribution. There is no way to get the ground-truth distribution. We choose to estimate it with sampling method. We count the frequency of operations in the architectures after architecture search and normalize it to get the approximate probability distribution. However, not all the architectures are equally important. We only use the architectures that belong to Pareto frontier. These architectures dominate all the other ones. Here, we say one architecture dominates the others if its latency is no bigger than others while its accuracy is no lower than others. Next, we remove the operations whose probability are below pre-defined threshold.

During CES, the architecture accuracy is predicted by supernet, which introduces error into the sorting part of CES, due to weight coupling. This implies Pareto frontier returned by CES is noisy, which may cause inaccurate estimation of operation probability distribution. To mitigate this effect, we count the frequency of operations from the architectures whose nondomination rank [12] is smaller than 10, where the nondomination rank of Pareto frontier is 1.

Pruned Supernet Training. After operation pruning, we get the pruned supernet. The training of pruned supernet is the same as initial supernet training. The only distinction is weights are randomly initialized in initial supernet training, while weights in the pruned supernet are inherited from the supernet in the previous stage. We only need to fine-tune the pruned supernet instead of training it from scratch. This reduces the search cost without affecting the performance.

4 Experiments

4.1 Dataset and Implement Details

Dataset. Throughout the paper, we use the ILSVRC2012 dataset [13]. ImageNet is a large-scale image dataset which contains over 1.2M training images and 50,000 validation images belonging to 1,000 classes. To be consistent with previous works, 50 images are randomly sampled from each class of the training set, and a total of 50,000 images are used as the validation set. The original validation set is used as the test set to measure the final performance of searched architecture.

Search Space. The whole network structure is shown in Table 1, which is used in previous work [5]. The search block structure (SBS) is the Inverted Bottleneck in MobileNetV2 [30].

For fair comparison, our basic search space is the same as ProxylessNAS [5], similar to FBNet [35], and shown in the left column of Table 2. The optional operations in each SBS are 6 types of operation (with a kernel size 3×3 , 5×5 or 7×7 and an expansion factor of 3 or 6), plus one identity operation. In addition, the expansion factor in the first SBS block is fixed as 1, and the identity operation is forbidden in the first layer of every block. The basic search space size is $3 \times 6^6 \times 7^{15} \approx 6.64 \times 10^{17}$.

Table 1. Architecture of the supernet. Output channels denotes the output channel number of a block. Repeat denotes the number of blocks in a stage. Stride denotes the stride of the first block in a stage. The output channel size of the first three stage is 32-16-32 in basic search space and 16-16-24 in large search space.

Input shape	Block	Output channels	Repeat	Stride
$224^2 \times 3$	3×3 conv	32 (16)	1	2
$112^2 \times 32$	SBS	16 (16)	1	1
$112^2 \times 16$	SBS	32 (24)	4	2
$56^2 \times 32$	SBS	40	4	2
$28^2 \times 40$	SBS	80	4	2
$14^2 \times 80$	SBS	96	4	1
$14^2 \times 96$	SBS	192	4	2
$7^2 \times 192$	SBS	320	1	1
$7^2 \times 320$	1×1 conv	1280	1	1
$7^2 \times 320$	global avgpool	-	1	1
$7^2 \times 1280$	fc	1000	1	-

Table 2. Operations table. IBConv_KX_EY represents the specific operator IBConv with expansion Y and kernel size X. IBConv denotes Inverted Bottleneck in MobilenetV2.

Basic search space	Operators exclusively in large search space	
IBConv_K3_E3	IBConv_K3_E1	IBConv_K5_E4
IBConv_K3_E6	IBConv_K3_E2	IBConv_K5_E5
IBConv_K5_E3	IBConv_K3_E4	IBConv_K7_E1
IBConv_K5_E6	IBConv_K3_E5	IBConv_K7_E2
IBConv_K7_E3	IBConv_K5_E1	IBConv_K7_E4
IBConv_K7_E6	IBConv_K5_E2	IBConv_K7_E5
Identity		

Moreover, we enlarge the search space by adding 12 more operations and formulate the large search space, as shown in the right column of right column of Table 2. We do not add any special operations, but a fine-grained version of the basic search space. In the basic search space, the expansion is either 3 or 6, while in the large search space, the expansion ranges from 1 to 6. The large search space size is $3 \times 18^6 \times 19^{15} \approx 1.55 \times 10^{27}$. The main reason we create this large search space here is to test whether HNAS can bridge the gap between theory that

larger search space brings better result for NAS and practice that larger search space causes more severe weight coupling.

Implementation Details. For the stand-alone training of the searched architecture (after evolutionary search) from scratch, we use the same settings (including data augmentation strategy, learning rate schedule, dropout rate etc.) as [15]. The network weights are optimized by momentum SGD, with an initial learning rate of 0.5, a momentum of 0.9, and a weight decay of 4×10^{-5} . A linear learning rate decay strategy is applied for 240 epochs and the batch size is 1024. It is worth noting that we have not used neither squeeze-and-excitation [19] nor swish activation functions [28]. Extra data augmentations such as mixup [37] and autoaugment [11] are not used as well.

For the training of the supernet, we first train the initial supernet for 120 epochs with an initial learning rate of 0.5. All other training settings are the same as stand-alone training. Next, we apply operation pruning for the first time and finetune the pruned supernet for 80 epochs with an initial learning rate of 0.1. Finally, we prune the operations for the second time and finetune the pruned supernet-2 for another 40 epochs with an initial learning rate of 0.1. The total number of supernet training epochs is 240, exactly the same as stand-alone training. Compared to [15], the architecture search in each operation pruning step is the only extra search cost, which is negligible, compared to supernet training,

For pruning the operation of the supernet, the pruning threshold P_{th} is set to 1% for each layer. And, the latency lower Lat_{min} and upper bound Lat_{max} is set to 60ms and 70ms for basic search space and 50ms and 100ms for large search space. The latency is measured on Pixel 3 using TFLite. The number of hierarchical search stages M is set to 4. In the constrained evolution search, the initial population size is set to 64, the max evolution iteration is set to 40, and the polynomial mutation and two-point crossover is adopted.

Notations. Two baseline methods are frequently mentioned in the following part. In the first baseline method, we fully train the initial supernet with single path and uniform sampling in [15] and search the architectures with CES proposed in this paper. We name it I-Supernet (Initial Supernet). I-Supernet is a special case of HNAS with $M = 2$ in Fig. 1 and Algorithm 1. There is no operation pruning inside. The second baseline method is called P-Supernet (Pruned Supernet). P-Supernet corresponds to HNAS with $M = 3$, where we only prune the operations once. HNAS denotes our main result, corresponding to HNAS with $M = 4$, where we prune the operations twice. I-Supernet-S, P-Supernet-S, and HNAS-S denote the corresponding method on the basic search space while I-Supernet-L, P-Supernet-L and HNAS-L represent the one on the large search space.

To make a fair comparison, for the three methods above, all the experimental setups are exactly the same, e.g., the total number of training epochs on ImageNet, learning rate, and hyperparameters in the CES. The only difference between these three methods is the number of hierarchical search stages M .

4.2 Comparison with State-of-the-art Methods

The experimental results are shown in Table 3. We compare our searched architectures with SOTA efficient architectures both designed automatically and manually. The primary metrics we care about are top-1 accuracy on the test set and mobile latency. If the latency is not available, the FLOPs is used as the secondary efficiency metric.

Table 3. Comparison with the state-of-the-arts on ImageNet under mobile setting.

No.	Model	Params	FLOPs	Latency	Top-1 Acc (%)	Top-5 Acc (%)
1	MobileNetV1 [18]	4.2M	569M	89.97ms	70.6	-
2	MobileNetV2 [30]	3.4M	300M	61.13ms	72.0	-
3	MobileNetV2 ($\times 1.4$) [30]	6.9M	585M	104.65ms	74.7	-
4	ShuffleNetV2 [25]	3.4M	299M	-	72.6	-
5	NASNet-mobile [41]	5.3M	564M	144.05ms	74.0	91.6
6	DARTS [22]	4.7M	574M	-	73.3	91.3
7	P-DARTS [7]	4.9M	574M	-	75.6	92.6
8	SPOS [15]	3.5M	319M	-	74.3	-
9	MnasNet [32]	4.2M	317M	64.24ms	74.0	91.8
10	Proxyless-R (mobile) [5]	4.1M	320M	67.66ms	74.6	92.2
11	FBNet-A [35]	4.3M	249M	54.05ms	73.0	-
12	FBNet-B [35]	4.5M	295M	63.79ms	74.1	-
13	FBNet-C [35]	5.5M	375M	79.18ms	74.9	-
14	Single Path NAS [31]	4.4M	334M	68.67ms	74.9	92.2
15	HNAS-S-A	3.7M	310M	61.31ms	74.6	91.9
16	HNAS-S-B	4.1M	315M	64.71ms	74.9	92.1
17	HNAS-S-C	4.2M	347M	69.85ms	75.2	92.3
18	HNAS-L-A	4.0M	271M	54.72ms	74.5	91.9
19	HNAS-L-B	4.2M	334M	67.23ms	75.2	92.4
20	HNAS-L-C	4.6M	385M	79.08ms	75.7	92.6
21	HNAS-L-D	4.6M	401M	90.21ms	75.9	92.6
22	HNAS-L-E	4.7M	444M	101.53ms	76.1	92.9

For the basic search space, we present three models HNAS-S-A, HNAS-S-B and HNAS-S-C according to their latency. Compared to manually designed network, as shown the first four rows in Table 3, it can reach significantly higher accuracy with lower latency(or FLOPs). In particular, HNAS-S-C achieves 75.2% with 69.85ms latency, which surpasses MobileNetV2(1.4X) top-1 accuracy by 0.4% while much faster (from 104.65ms to 69.85ms). Compared with Proxyless-R [5] which shares exactly the same search space, ours HNAS-S-B improves the accuracy by 0.3% but still faster (2.95ms less for processing single image on Pixel 3). Finally, in comparison with other SOTA NAS algorithms, the three models all achieve higher accuracy with lower latency.

For the large search space, we list five models according to their latency, named HNAS-L-A, HNAS-L-B, HNAS-L-C, HNAS-L-D and HNAS-L-E, whose detailed architectures are illustrated in Fig. 4. The top-1 accuracy of HNAS-L-A is 74.5%, which is 1.5% higher than its counterpart FBNet-A [35]. HNAS-L-B achieves 75.2% top-1 accuracy, which is 0.6% higher than Proxyless-R [5],

and exhibits the same accuracy as HNAS-S-C with lower latency. HNAS-L-C achieves 75.7% top-1 accuracy, 0.8% higher than FBNet-C [35]. These results demonstrate our proposed HNAS can be applied to larger search space, and achieve even better performance.

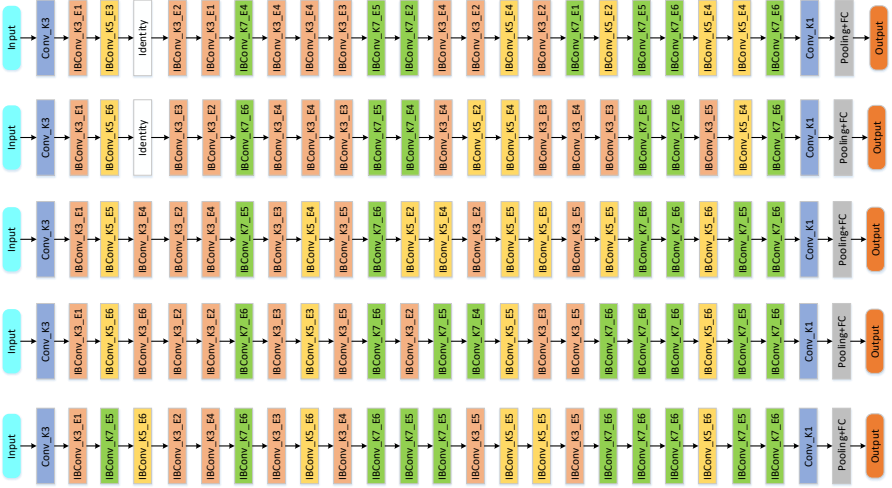


Fig. 4. Architectures of HNAS-L-A,B,C,D,E in Fig. 2 (from top to bottom).

4.3 Ablation Studies

Two baseline methods are mentioned in this part, I-Supernet and P-Supernet, whose corresponding description can be found in **Notations** of Sec. 4.1.

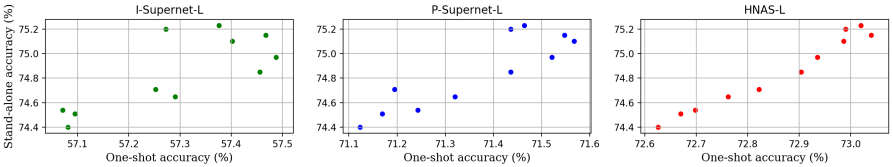


Fig. 5. Top-1 accuracy of 11 stand-alone trained architectures vs. one-shot models.

Kendall Rank Analysis and Comparison. The ranking consistency of stand-alone and one-shot model accuracy is an important problem in One-Shot NAS algorithm. It indicates whether supernet can reflect the relative performance of models. Due to high training cost, we sample 11 models at approximately equal distances on the Pareto frontier and do the stand-alone training from scratch to get the ranking, as shown in Fig. 5. We can observe in HNAS-L, one-shot accuracy is more relevant to stand-alone accuracy, compared to the baseline method I-Supernet-L where there is no operation pruning involved.

We also use Kendall’s rank correlation coefficient τ [20] to measure this consistency. τ ranges from -1 to 1, meaning the rankings are totally reversed or completely preserved, whereas 0 means there is no correlation at all. As shown in Table 4, as the number of hierarchical search stage M increases, the spaces size is reduced dramatically by orders-of-magnitude, and Kendall’s ranking coefficient τ has significantly increased from 0.48 to 0.92.

Table 4. Ranking consistency comparison with baseline methods. Size represents search space size.

Algorithm	τ	Size	M
I-Supernet-L	0.48	10^{27}	2
P-Supernet-L	0.66	10^{15}	3
HNAS-L	0.92	10^9	4

Table 5. Performance comparison between I-Supernet and HNAS on different search spaces. Stand-alone Top-1 Acc means the best top-1 accuracy of searched architecture when stand-alone trained from scratch under the same latency(69ms).

Algorithm	Supernet Top-1 Acc (%)	Stand-alone Top-1 Acc (%)
I-Supernet-L	52.3	74.4
HNAS-L	72.4	75.4
I-Supernet-S	65.5	74.8
HNAS-S	71.4	75.2

Impact of Search Space. Theoretically, NAS should give better result when larger search space is used. However, as stated in Table 5, I-Supernet-L achieves even lower stand-alone top-1 accuracy than I-Supernet-S. There exists a gap between theory and practice in current one-shot approaches. More operations brings more intense interference between operations during the training of supernet, which makes the weight coupling more severe. Thanks to the proposed hierarchical search strategy, HNAS-L performs better than HNAS-S, which implies HNAS can bridge this gap. Besides, we can see top-1 accuracy achieved by HNAS-L is 1.0% higher than I-Supernet-L while this number is only 0.4% for basic search space. This shows the advantage of HNAS is more obvious in larger search space. We can also notice big gap exists between supernet accuracy and stand-alone one in the baseline method I-Supernet, as large as 20%, while this gap is much lower in HNAS, only 3%. We also present the corresponding supernet accuracy curve on validation dataset for HNAS and I-Supernet in Fig. 6. The supernet accuracy of I-Supernet-L is always below I-Supernet-S. Similar trend also exists in the first 120 epochs of H-NAS. However, once operation pruning is introduced, the gap between HNAS-L and HNAS-S is becoming much smaller. And HNAS-L eventually surpasses HNAS-S at epoch 240 after we prune the operations twice.

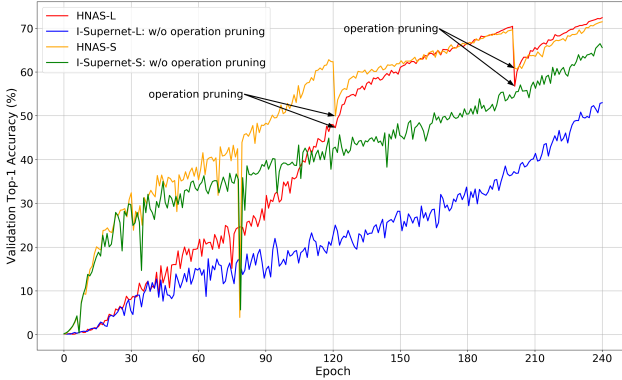


Fig. 6. Supernet accuracy curve comparison between I-Supernet and HNAS.

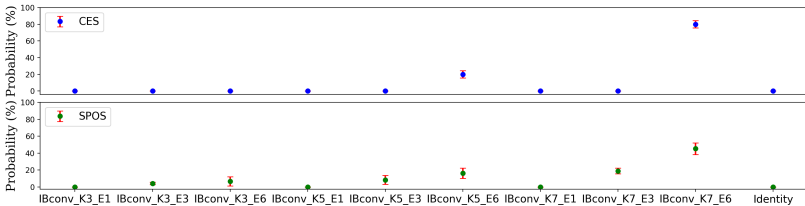


Fig. 7. Estimated probability distribution of the operations in the last layer by CES and SPOS [15], respectively.

Impact of Evolutionary Algorithm. We study the impact of different evolutionary algorithms on the estimated probability distribution of operations. Two algorithms are compared here: one is our CES while the other is the one used in SPOS [15]. Each algorithm is repeated 5 times with different random seeds to get the mean and variance of estimated distribution. As illustrated in Fig. 7, the result of our CES exhibits a much lower variance than SPOS [15], which indicates CES gives us more stable result. Besides, the distribution corresponding to CES is sparser than SPOS, which makes operation pruning more efficient.

5 Conclusion

In this paper, we present HNAS, a hierarchical search strategy for One-Shot NAS. It automatically builds a layer-wise operation search space through hierarchical operation pruning. The target device latency constraint is incorporated into the search for efficient model deployment. HNAS mitigates weight coupling issue in One-Shot NAS and significantly improves the ranking consistency between supernet predicted accuracy and stand-alone trained accuracy. Experimental results demonstrate the effectiveness of our method, which achieves SOTA performance on ImageNet.

References

1. Abadi, M., Agarwal, A., Barham, P., Brevdo, E., Chen, Z., Citro, C., Corrado, G.S., Davis, A., Dean, J., Devin, M., et al.: Tensorflow: Large-scale machine learning on heterogeneous distributed systems. arXiv preprint arXiv:1603.04467 (2016) [3](#)
2. Adam, G., Lorraine, J.: Understanding neural architecture search techniques. arXiv preprint arXiv:1904.00438 (2019) [2](#)
3. Bender, G., Kindermans, P.J., Zoph, B., Vasudevan, V., Le, Q.V.: Understanding and simplifying one-shot architecture search. In: ICML (2018) [2](#), [4](#), [5](#), [7](#)
4. Brock, A., Lim, T., Ritchie, J.M., Weston, N.J.: Smash: One-shot model architecture search through hypernetworks. In: ICLR (2018) [1](#), [2](#), [4](#), [5](#), [7](#)
5. Cai, H., Zhu, L., Han, S.: ProxylessNAS: Direct neural architecture search on target task and hardware. In: ICLR (2019) [1](#), [3](#), [4](#), [8](#), [9](#), [11](#)
6. Chen, W., Gong, X., Liu, X., Zhang, Q., Li, Y., Wang, Z.: Fasterseg: Searching for faster real-time semantic segmentation. In: ICLR (2020) [1](#)
7. Chen, X., Xie, L., Wu, J., Tian, Q.: Progressive darts: Bridging the optimization gap for nas in the wild. arXiv preprint arXiv:1912.10952 (2019) [11](#)
8. Chen, X., Xie, L., Wu, J., Tian, Q.: Progressive differentiable architecture search: Bridging the depth gap between search and evaluation. In: ICCV (2019) [4](#)
9. Chen, Y., Yang, T., Zhang, X., Meng, G., Xiao, X., Sun, J.: Detnas: Backbone search for object detection. In: NeurIPS. pp. 6638–6648 (2019) [1](#)
10. Chu, X., Zhang, B., Xu, R., Li, J.: Fairnas: Rethinking evaluation fairness of weight sharing neural architecture search. arXiv preprint arXiv:1907.01845 (2019) [2](#), [4](#)
11. Cubuk, E.D., Zoph, B., Mane, D., Vasudevan, V., Le, Q.V.: Autoaugment: Learning augmentation strategies from data. In: CVPR (2019) [10](#)
12. Deb, K.: A fast elitist non-dominated sorting genetic algorithm for multi-objective optimization: Nsga-2. IEEE Trans. Evol. Comput. **6**(2), 182–197 (2002) [7](#), [8](#)
13. Deng, J., Dong, W., Socher, R., Li, L.J., Li, F.F.: Imagenet: a large-scale hierarchical image database. In: CVPR (2009) [8](#)
14. Fleischer, M.: The measure of pareto optima applications to multi-objective metaheuristics. In: International Conference on Evolutionary Multi-Criterion Optimization. pp. 519–533. Springer (2003) [3](#)
15. Guo, Z., Zhang, X., Mu, H., Heng, W., Liu, Z., Wei, Y., Sun, J.: Single path one-shot neural architecture search with uniform sampling. arXiv preprint arXiv:1904.00420 (2019) [1](#), [2](#), [3](#), [4](#), [5](#), [6](#), [7](#), [10](#), [11](#), [14](#)
16. Han, S., Mao, H., Dally, W.J.: Deep compression: Compressing deep neural networks with pruning, trained quantization and huffman coding. In: ICLR (2016) [4](#), [5](#)
17. He, Y., Zhang, X., Sun, J.: Channel pruning for accelerating very deep neural networks. In: ICCV (2017) [4](#)
18. Howard, A.G., Zhu, M., Chen, B., Kalenichenko, D., Wang, W., Weyand, T., Andreetto, M., Adam, H.: Mobilenets: Efficient convolutional neural networks for mobile vision applications. arXiv preprint arXiv:1704.04861 (2017) [11](#)
19. Hu, J., Shen, L., Sun, G.: Squeeze-and-excitation networks. In: CVPR (2018) [10](#)
20. Kendall, M.G.: A new measure of rank correlation. Biometrika **30**(1/2), 81–93 (1938) [13](#)
21. Liu, C., Chen, L.C., Schroff, F., Adam, H., Hua, W., Yuille, A.L., Fei-Fei, L.: Auto-deeplab: Hierarchical neural architecture search for semantic image segmentation. In: CVPR (2019) [1](#)

22. Liu, H., Simonyan, K., Yang, Y.: Darts: Differentiable architecture search. In: ICLR (2019) [1](#), [4](#), [7](#), [11](#)
23. Liu, Z., Li, J., Shen, Z., Huang, G., Yan, S., Zhang, C.: Learning efficient convolutional networks through network slimming. In: ICCV (2017) [4](#)
24. Lu, Z., Whalen, I., Boddeti, V., Dhebar, Y., Deb, K., Goodman, E., Banzhaf, W.: Nsga-net: neural architecture search using multi-objective genetic algorithm. In: Proceedings of the Genetic and Evolutionary Computation Conference. pp. 419–427. ACM (2019) [7](#)
25. Ma, N., Zhang, X., Zheng, H.T., Sun, J.: Shufflenet v2: Practical guidelines for efficient cnn architecture design. In: ECCV. pp. 116–131 (2018) [11](#)
26. Nekrasov, V., Chen, H., Shen, C., Reid, I.: Fast neural architecture search of compact semantic segmentation models via auxiliary cells. In: CVPR (2019) [1](#)
27. Pham, H., Guan, M.Y., Zoph, B., Le, Q.V., Dean, J.: Efficient neural architecture search via parameter sharing. In: ICML (2018) [1](#), [4](#)
28. Ramachandran, P., Zoph, B., Le, Q.V.: Searching for activation functions. arXiv preprint arXiv:1710.05941 (2017) [10](#)
29. Real, E., Aggarwal, A., Huang, Y., Le, Q.V.: Regularized evolution for image classifier architecture search. In: Proceedings of the aaai conference on artificial intelligence. vol. 33, pp. 4780–4789 (2019) [1](#)
30. Sandler, M., Howard, A., Zhu, M., Zhmoginov, A., Chen, L.C.: Mobilenetv2: Inverted residuals and linear bottlenecks. In: CVPR (2018) [3](#), [8](#), [11](#)
31. Stamoulis, D., Ding, R., Wang, D., Lymberopoulos, D., Priyantha, B., Liu, J., Marculescu, D.: Single-path nas: Designing hardware-efficient convnets in less than 4 hours. arXiv preprint arXiv:1904.02877 (2019) [11](#)
32. Tan, M., Chen, B., Pang, R., Vasudevan, V., Sandler, M., Howard, A., Le, Q.V.: Mnasnet: Platform-aware neural architecture search for mobile. In: CVPR (2019) [11](#)
33. Tan, M., Pang, R., Le, Q.V.: Efficientdet: Scalable and efficient object detection. arXiv preprint arXiv:1911.09070 (2019) [1](#)
34. Williams, R.J.: Simple statistical gradient-following algorithms for connectionist reinforcement learning. *Machine learning* **8**(3-4), 229–256 (1992) [1](#)
35. Wu, B., Dai, X., Zhang, P., Wang, Y., Sun, F., Wu, Y., Tian, Y., Vajda, P., Jia, Y., Keutzer, K.: Fbnet: Hardware-aware efficient convnet design via differentiable neural architecture search. In: CVPR (2019) [1](#), [3](#), [4](#), [9](#), [11](#), [12](#)
36. Xie, S., Zheng, H., Liu, C., Lin, L.: Snas: stochastic neural architecture search. arXiv preprint arXiv:1812.09926 (2018) [1](#)
37. Zhang, H., Cisse, M., Dauphin, Y.N., Lopez-Paz, D.: mixup: Beyond empirical risk minimization. In: ICLR (2018) [10](#)
38. Zhang, L.L., Yang, Y., Jiang, Y., Zhu, W., Liu, Y.: Integrating hardware diversity with neural architecture search for efficient convolutional neural networks. arXiv preprint arXiv:1910.11609 (2019) [4](#)
39. Zhang, X., Huang, Z., Wang, N.: You only search once: Single shot neural architecture search via direct sparse optimization. arXiv preprint arXiv:1811.01567 (2018) [1](#)
40. Zoph, B., Le, Q.V.: Neural architecture search with reinforcement learning. In: ICLR (2017) [1](#)
41. Zoph, B., Vasudevan, V., Shlens, J., Le, Q.V.: Learning transferable architectures for scalable image recognition. In: CVPR (2018) [1](#), [11](#)